Neurosci. Bull. June, 2018, 34(3):465–475
https://doi.org/10.1007/s12264-018-0211-0

www.neurosci.cn
www.springer.com/12264

ORIGINAL ARTICLE

Dendritic Cell Factor 1-Knockout Results in Visual Deficit Through the GABA System in Mouse Primary Visual Cortex

Jieyun Shi[1] · Qian Li[1] · Tieqiao Wen[1]

Received: 8 August 2017 / Accepted: 21 November 2017 / Published online: 12 February 2018

Abstract The visual system plays an important role in our daily life. In this study, we found that loss of dendritic cell factor 1 (DCF1) in the primary visual cortex (V1) caused a sight deficit in mice and induced an abnormal increase in glutamic acid decarboxylase 67, an enzyme that catalyzes the decarboxylation of glutamate to gamma aminobutyric acid and CO_2, particularly in layer 5. *In vivo* electrophysiological recordings confirmed a decrease in delta, theta, and beta oscillation power in DCF1-knockout mice. This study presents a previously unknown function of DCF1 in V1, suggests an unknown contact between DCF1 and GABA systems, and provides insight into the mechanism and treatment of visual deficits.

Keywords DCF1 · Sight · GABA · GAD67

Introduction

Vision plays an important role in daily life. A visual deficit can be caused by a variety of factors, and the structure and function of the primary visual cortex (V1) are fundamental aspects of the visual system. Experience-dependent modification of visual cortical function is based on the plasticity of excitatory and inhibitory synapses [1]. Gamma aminobutyric acid (GABA) is the main inhibitory neurotransmitter in the adult mammalian brain [2]. Information-processing in sensory cortex relies on interactions between excitatory and inhibitory circuits, mediated by a diversity of GABAergic interneurons [3]. Abnormal GABA levels can result in electrophysiological abnormalities. GABA is synthesized by the glutamic acid decarboxylases GAD67 and GAD65 (encoded by the Gad1 and Gad2 genes, respectively) [4]. GABA synthesis is the rate-limiting step in GABA metabolism [5]. Between the two isoforms, GAD67 is responsible for >90% of the basal GABA synthesis and its production is limited in the brain [6]. The level of GAD67 essentially reflects the activity of GABAergic neurons.

Dendritic cell factor 1 (DCF1, also known as TMEM59), is a protein consisting of 323 amino-acids. It is composed of an N-terminal signal sequence, a mitochondrial-targeting sequential motif, a transmembrane region, and a cytoplasmic tail [7]. Our previous study showed that DCF1 is involved in the differentiation of neural stem cells [8], as silencing DCF1 tends to reduce the generation of neurons [9, 10]. Our study on DCF1-knockout mouse revealed developmental disorders of dendritic spines in hippocampal synapses [7]. In the present study, we found that DCF1-knockout (KO) mice had visual impairment, and therefore hypothesized that the lack of DCF1 affects neurons in V1, resulting in a visual deficit. We tested this hypothesis and found that the visual impairment in DCF1-KO mice was mediated by the GABA system.

Electronic supplementary material The online version of this article (https://doi.org/10.1007/s12264-018-0211-0) contains supplementary material, which is available to authorized users.

✉ Tieqiao Wen
wtq@shu.edu.cn

[1] Laboratory of Molecular Neural Biology, School of Life Sciences, Shanghai University, 333 Nanchen Road, Shanghai 200444, China

Material and Methods

Animals and Drug Treatment

C57BL/6 mice were housed at 23°C with food and water *ad libitum*. All experiments were performed in a quiet room between 09:00 and 15:00. Test mice were habituated to the testing room for at least 1 h before experiments. All animal protocols were approved by the Shanghai University Ethics Committee.

Drug Treatment

Mice in the treatment group were injected intraperitoneally with Ginkgolide A at 10 mg/kg body weight diluted with dimethylsulfoxide (DMSO) and normal saline for 5 consecutive days, while mice in the control group were injected intraperitoneally with an equal volume of DMSO and normal saline.

Animal Behavior

Head-Tracking Assay

Head-tracking was assayed in a visual tracking drum (Fig. 1A). Each mouse was placed on the platform and allowed to settle for 30 s. When the motor was started, it drove the hollow cylinder with black-and-white stripes, and the mouse was video-recorded for head-tracking responses (defined as a horizontal head movement at the same rate and in the same direction as the drum for at least 15°) [11]. The video was assessed after the test, and the behavior was scored.

Morris Water Maze Test

The Morris water maze test was conducted in a pool full of water with a white edible pigment and a platform above the surface. Test animals were trained by being placed in the pool from a random location three times per day for 3 days and allowed to swim to a platform. A test animal was introduced into the pool from the far side (position F in Fig. 1C). The time the mouse took to swim from the entry position to the platform was measured. Then, the test animal was introduced into the pool from the near side (position C in Fig. 1C) for a second run.

Western Blot

Tissue samples were lysed in protein lysis buffer, and 10–15 μg protein was loaded into each lane for sodium dodecyl sulfate-polyacrylamide gel electrophoresis. The nitrocellulose membrane was blocked with 5% bovine serum albumin (BSA) and incubated with primary antibodies [anti-GAPDH (1:1000, Santa Cruz Biotechnology, Santa Cruz, CA), anti-GAD67 (MAB5406; 1:1000, Millipore, Billerica, MA), anti-glutamine synthetase (MAB302; 1:1000, Millipore), and anti-choline acetyltransferase (AB144P; 1:1000, Millipore)]. After washing three times (5 min each), the membrane was incubated with secondary antibody, and the blot was imaged using the LI-COR Odyssey system (Gene Company Limited, USA).

Immunohistochemistry and Visual Activation

All mice were deeply anesthetized and transcardially perfused with phosphate-buffered saline (PBS) followed by 4% paraformaldehyde. The fixed brains were removed and kept in 4% paraformaldehyde at 4°C for 12 h. Then, they were moved to 20% sucrose in 0.01 mol/L PBS for 12 h, followed by 30% sucrose in PBS for 3 days. Frozen sections were then cut at 20 μm. The sections were washed several times in PBS before they were permeabilized and blocked for 1 h in PBS containing 5% BSA and 0.2% Triton X-100. The sections were incubated overnight at 4°C in PBS containing 0.1% Triton X-100 with the primary antibodies. The sections were incubated simultaneously with two primary antibodies for the double-labeling experiments. After a thorough wash in PBS, the sections were incubated with the secondary antibody diluted in PBS for 2 h, and with 0.01% DAPI in PBS for 10 min. The sections were then washed repeatedly with PBS and coverslipped [12].

For visual activation, daylight was simulated using an LED to provide white light at 3 lux. After adapting in the dark for one week, mice were exposed to light for 1 h to activate the visual signaling pathways.

Surgery and Electrophysiological Recording

Stereotactic surgery was performed under anesthesia (each mouse was intraperitoneally injected with 150 μL of 2% pentobarbital sodium). A custom-made head-stage was attached to the skull using a dental resin. We marked the corresponding stereotactic coordinates for V1 during the surgery for later targeting of recordings. All recordings were made in conscious mice using a single electrode (Plexon Inc., Dallas, TX). The electrode was slowly inserted into V1 [coordinates (in mm) –3.2 AP, 2.0 ML, 0.8 depth] at 1 μm/s–2 μm/s. The top electrode contact was positioned just below the brain surface, and the deepest contact was ~1.0 mm from the surface.

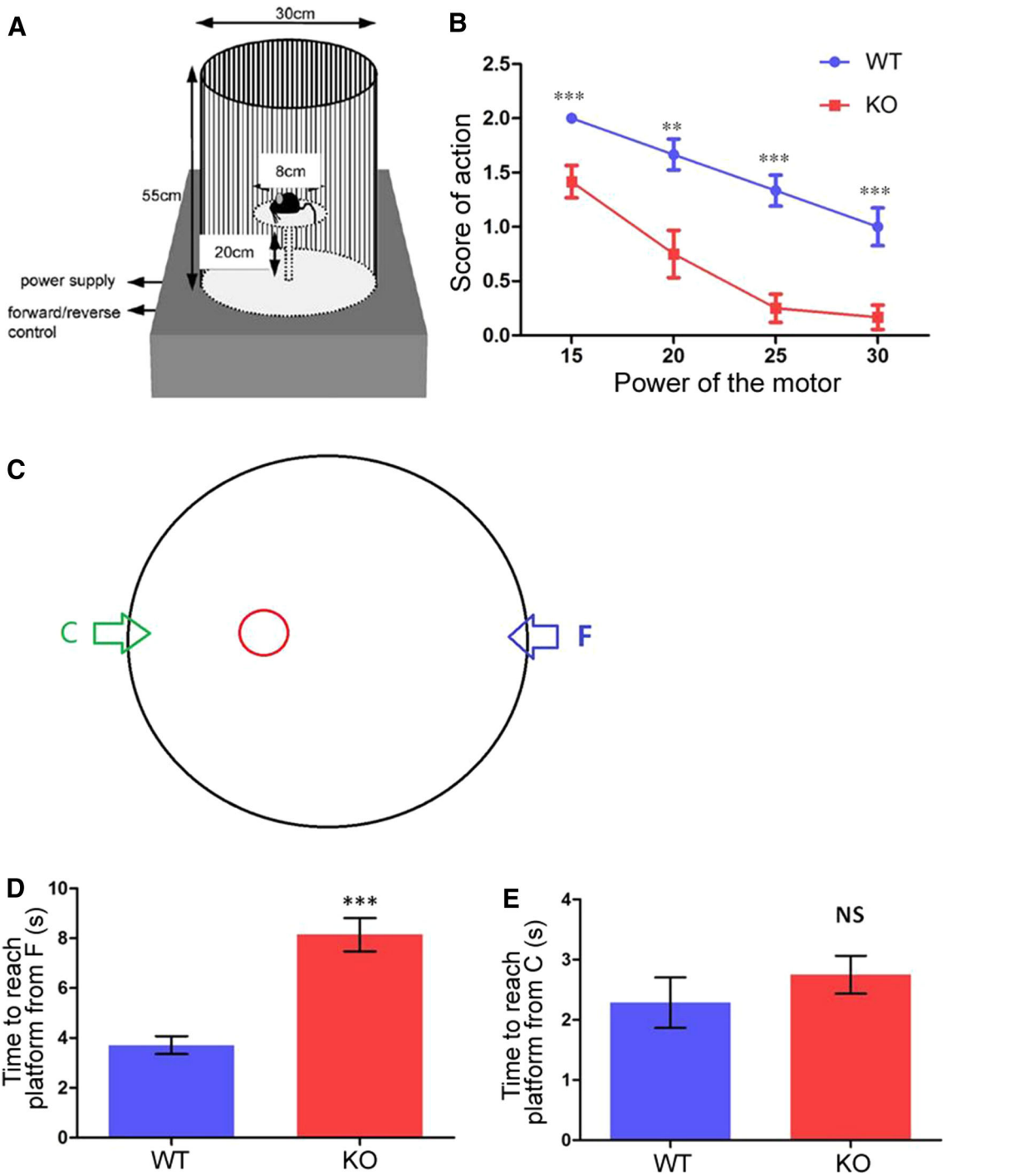

Fig. 1 Dendritic cell factor-knockout (DCF1-KO) mice have a visual deficit. **A** Schematic of the visual tracking assay. **B** DCF1-KO mice showed a low score on visual tracking (**$P < 0.01$, ***$P < 0.001$, one-way ANOVA, mean ± standard error (SE); $n = 12$). **C** Schematic of visual water test. **D**, **E** Time taken by DCF1-KO mice to reach the platform from the far side at position F was longer than that of wild-type (WT) mice, but the times to reach the platform from the near side at position C were similar in the two groups (***$P < 0.001$, NS, not significant, one-way ANOVA; mean ± SEM; $n = 7$).

V1 recordings were performed using a multichannel recording system (Plexon OmniPlex OPX-D-170). Local field potentials (LFPs) were low-pass filtered at 3 kHz and high-pass filtered at 0.5 Hz. Recordings with visual stimulation were made in the dark.

Electrophysiological Data Analysis

All data were analyzed using MATLAB (MathWorks, Natick, MA). LFPs were first bandpass filtered at 0.5–500 Hz with a second-order Butterworth filter to eliminate low-

frequency drift, and then down-sampled to 250 Hz using the resample function in MATLAB. The resulting LFPs were passed through a 50-Hz notch filter using iirnotch in MATLAB. To reduce edge artifacts, 300 ms of data was removed from the beginning and end of each trial in all subsequent analysis.

Spectral Analysis

We used the multitaper Fourier method for all spectral analysis, because it reduces noise through spectral smearing by obtaining multiple independent estimates from the data. Spectra and spectrograms were calculated using the mtspectrumc and mtspecgramc functions in the Chronux toolbox [13]. The power spectrogram was described by a Poisson distribution.

Statistical Analysis

Data are expressed as mean ± standard error. Student's *t*-test was used to assess differences between two groups and one-way analysis of variance (ANOVA) was used for more than two groups. A *P*-value <0.05 was considered significant.

Results

DCF1-KO Mice Have a Visual Deficit

We had previously found that the vision of DCF1-KO mice was poorer than that of wild-type (WT) mice, so we conducted two behavioral tests. The first was the head-tracking assay used by Thomas and Thaung [11], in which a

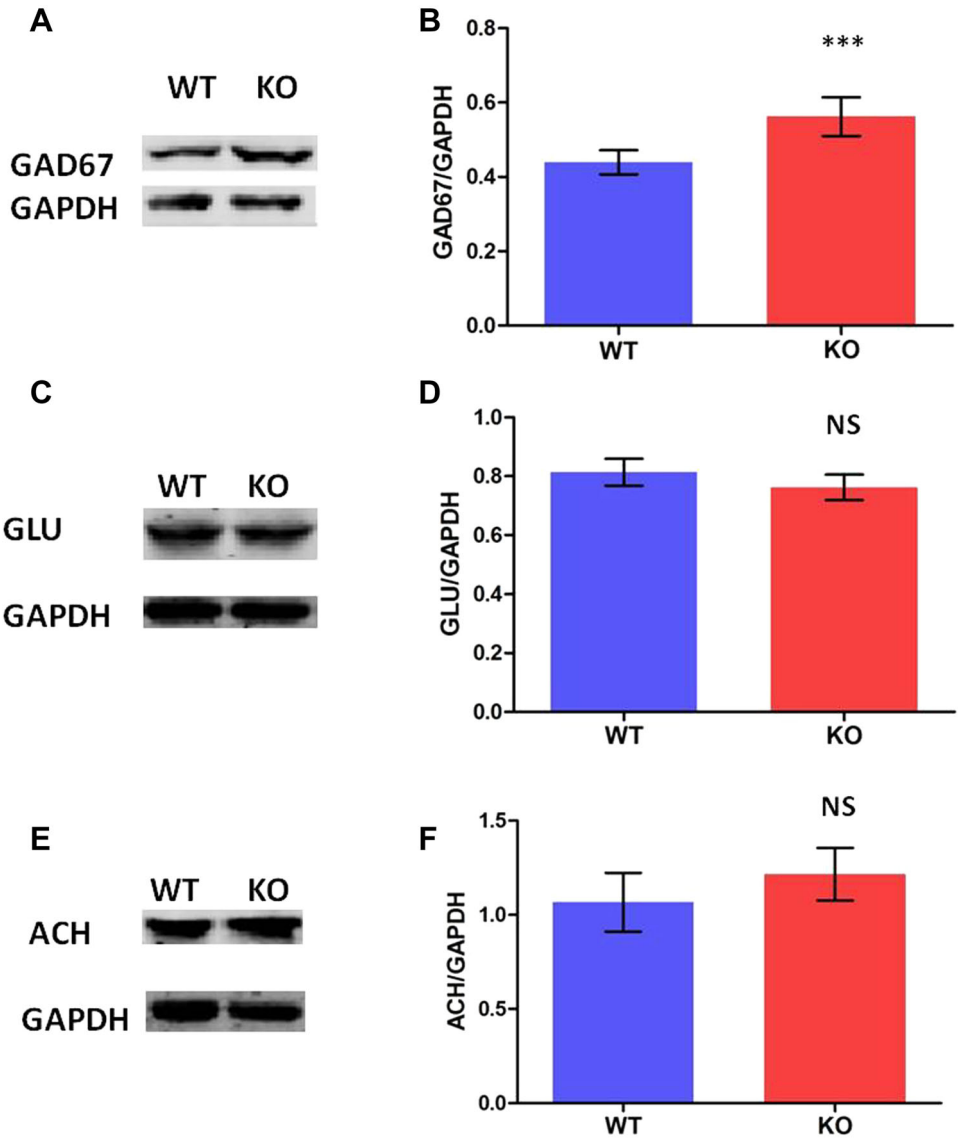

Fig. 2 DCF1-KO mice have more GAD67 in the primary visual cortex. **A**–**F** Western blotting of V1 from DCF1-KO and wild-type (WT) mice (**A**, **C**, **E**). The expression level of GAD67 was higher in the DCF1-KO mice than in the WT mice (**B**, **D**, **F**; ***$P < 0.001$, one-way ANOVA; mean ± SE; $n = 4$).

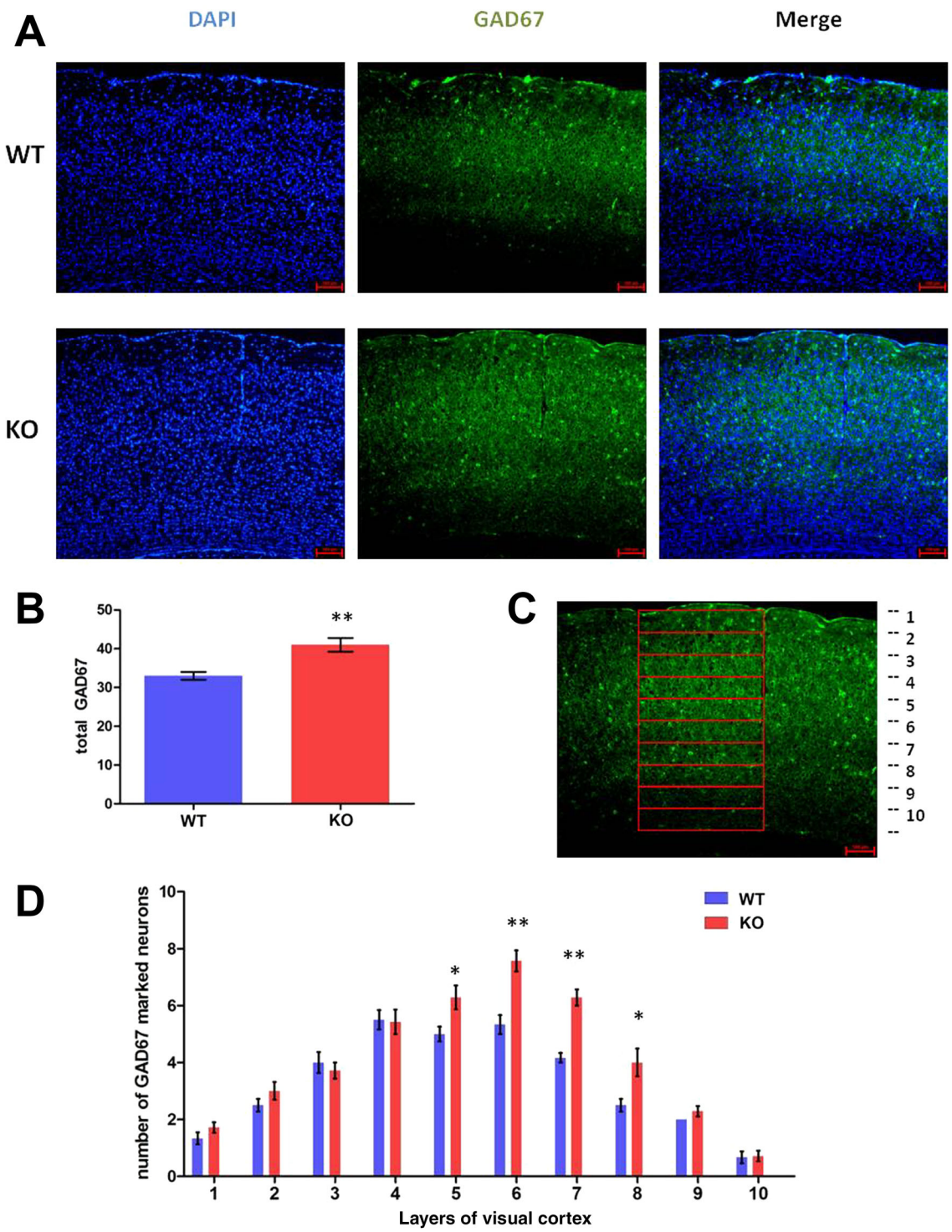

Fig. 3 Dendritic cell factor-knockout (DCF1-KO) mice show high levels of GABA in layers 4 and 5 of the primary visual cortex. **A** Fluorescence micrographs of neurons labeled with GAD67 (green) and DAPI (blue) in V1. Scale bar 100 μm. **B** The total number of GAD67-labeled neurons in V1 of DCF1-KO mice was greater than in WT mice (**$P < 0.01$, one-way ANOVA; mean ± SE; $n = 6$). **C** Image showing cortex divided into 10 layers. Scale bar 100 μm. **D** The number of GAD67-labeled neurons in DCF1-KO mice was greater than in WT mice in layers 5–8 (*$P < 0.05$, **$P < 0.01$, one-way ANOVA; mean ± SE; $n = 6$).

mouse is placed in a visual tracking drum, and its head movements are monitored (Fig. 1A). Video recordings have shown that the head-tracking response is able to differentiate between mice that can see normally and those that have a severe loss of visual function [11]. In this test, DCF1-KO mice had lower scores than WT mice (Fig. 1B). The second was the Morris water maze test, in which a mouse is required to locate a platform in a water tank, starting from different locations (Fig. 1C). The results showed that DCF1-KO mice needed more time to reach the platform from the far side than the WT mice, whereas the two groups took similar times to reach the platform from the near side (Fig. 1D, E). Taken together, these results confirmed that the vision of DCF1-KO mice is poorer than that of WT mice.

DCF1-KO Mice Have Higher GAD67 Levels in the Primary Visual Cortex

No differences in the whole retina, outer nuclear layer, or inner nuclear layer thickness were detected between the WT and DCF1-KO mice (Fig. S1A–C). Since it has been reported that glutamatergic, GABAergic, and cholinergic signaling

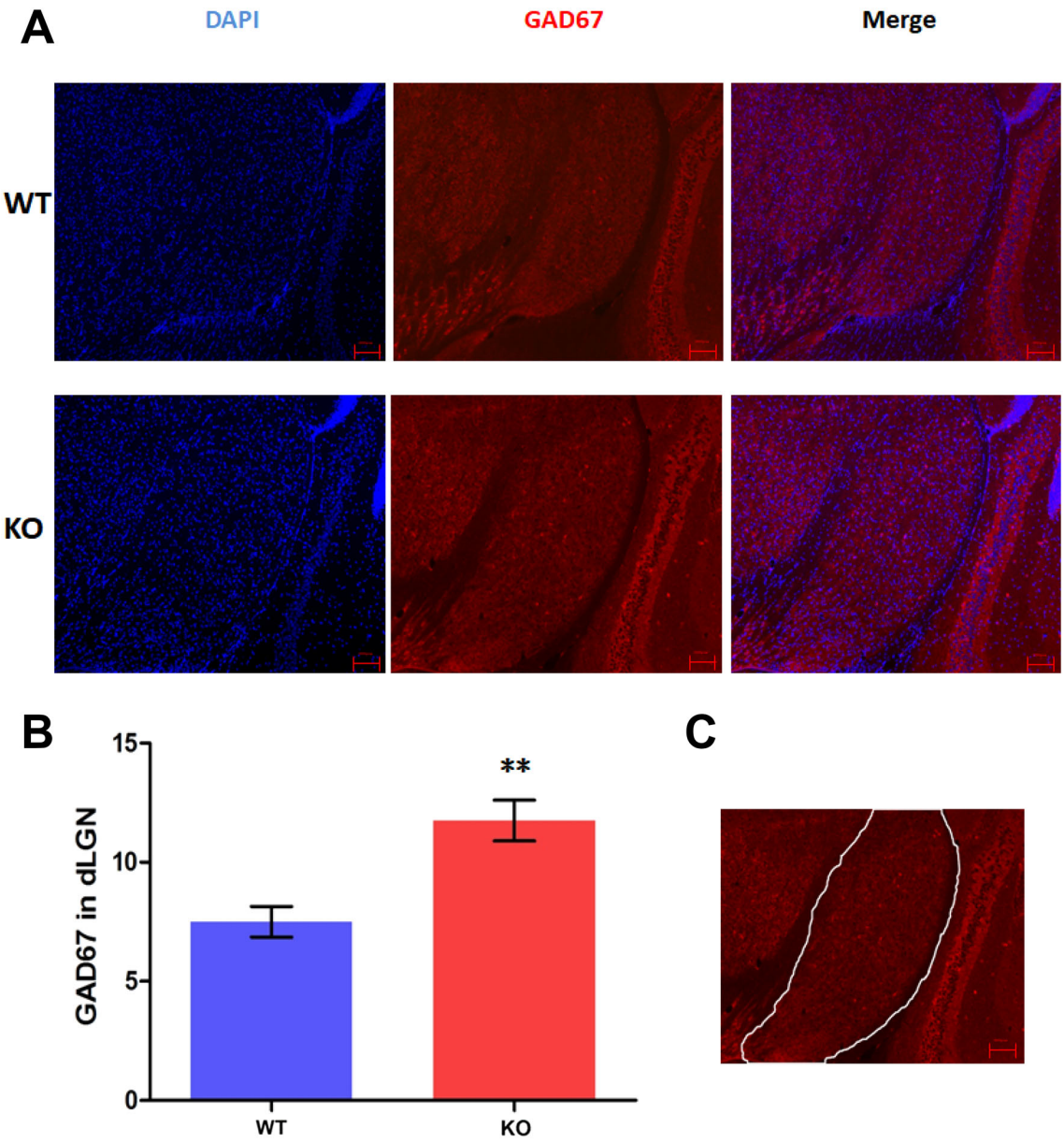

Fig. 4 DCF1-KO mice show more GAD67 in the lateral geniculate nucleus. **A** Fluorescence micrographs of neurons labeled with GAD67 (red) and DAPI (blue) in the LGN. Scale bar, 100 μm. **B** The number of GAD67-labeled neurons in the LGN of DCF1-KO mice was greater than that in WT mice, (**$P < 0.01$, one-way ANOVA; mean ± SE; $n = 6$). **C** LGN (outlined) stained for GAD67 (red). Scale bar, 100 μm.

play important roles in neuronal signaling [14–16], we assessed the functional neurons in V1, and found that the level of GAD67 was significantly higher (Fig. 2A, B), while the levels of glutamine synthetase (Fig. 2C, D) and anti-choline acetyltransferase (Fig. 2E, F) were similar to the WT.

DCF1-KO Mice Express More GAD67 in Layer 5 of Primary Visual Cortex

We used immunohistochemistry to determine the distribution of GABAergic neurons in V1 (Fig. 3A). The total number of GAD67-labeled neurons was higher than in WT mice, confirming that more GABAergic neurons were present in DCF1-KO mice than in WT mice (Fig. 3B). Dividing the cortex into 10 layers, the increase in GAD67 was distributed in layers 5–8 (Fig. 3C, D). What is more, it has been reported that the synthesis and signaling regulation of GABA mediated by GAD67 play important roles in visual cortex [17]. The increase in GAD67 in the DCF1-KO mice supports the notion that more GABAergic neurons are present mainly in layer 5 of V1.

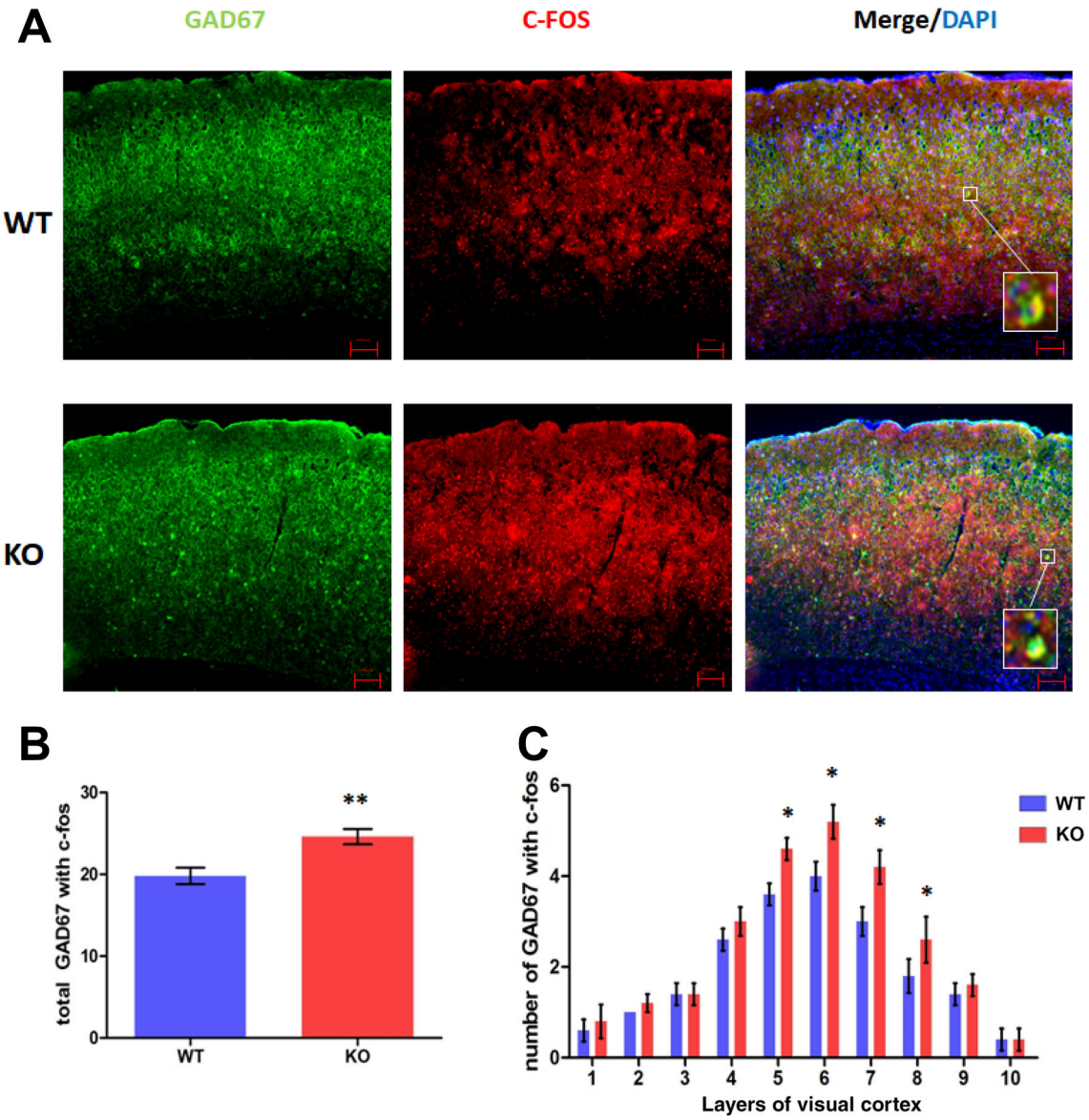

Fig. 5 DCF1-KO mice show high levels of visually-activated GABAergic neurons in layer 5 of primary visual cortex. **A** Fluorescence micrographs of neurons labeled with GAD67 (green), c-fos (red), and DAPI (blue) in V1 (the amplified area showed their co-localization). Scale bars: 100 μm. **B** The total number of GAD67 and c-fos co-labeled neurons in V1 of DCF1-KO mice was greater than that in WT mice (**$P < 0.01$, one-way ANOVA; mean ± SE; $n = 6$). (**C**) Dividing the primary visual cortex into 10 layers, we found that the number of GAD67 and c-fos co-labeled neurons in DCF1-KO mice was higher than that in WT mice in layers 5–8 (*$P < 0.05$, one-way ANOVA; mean ± SE; $n = 6$).

DCF1-KO Mice Have More GAD67 in the Lateral Geniculate Nucleus

Since the lateral geniculate nucleus (LGN) is a thalamic relay in the visual pathway, we further investigated the expression of GAD67 in this area (Fig. 4A). The results showed a significant increase of GAD67 in the DCF1-KO mice, consistent with the findings above (Fig. 4B).

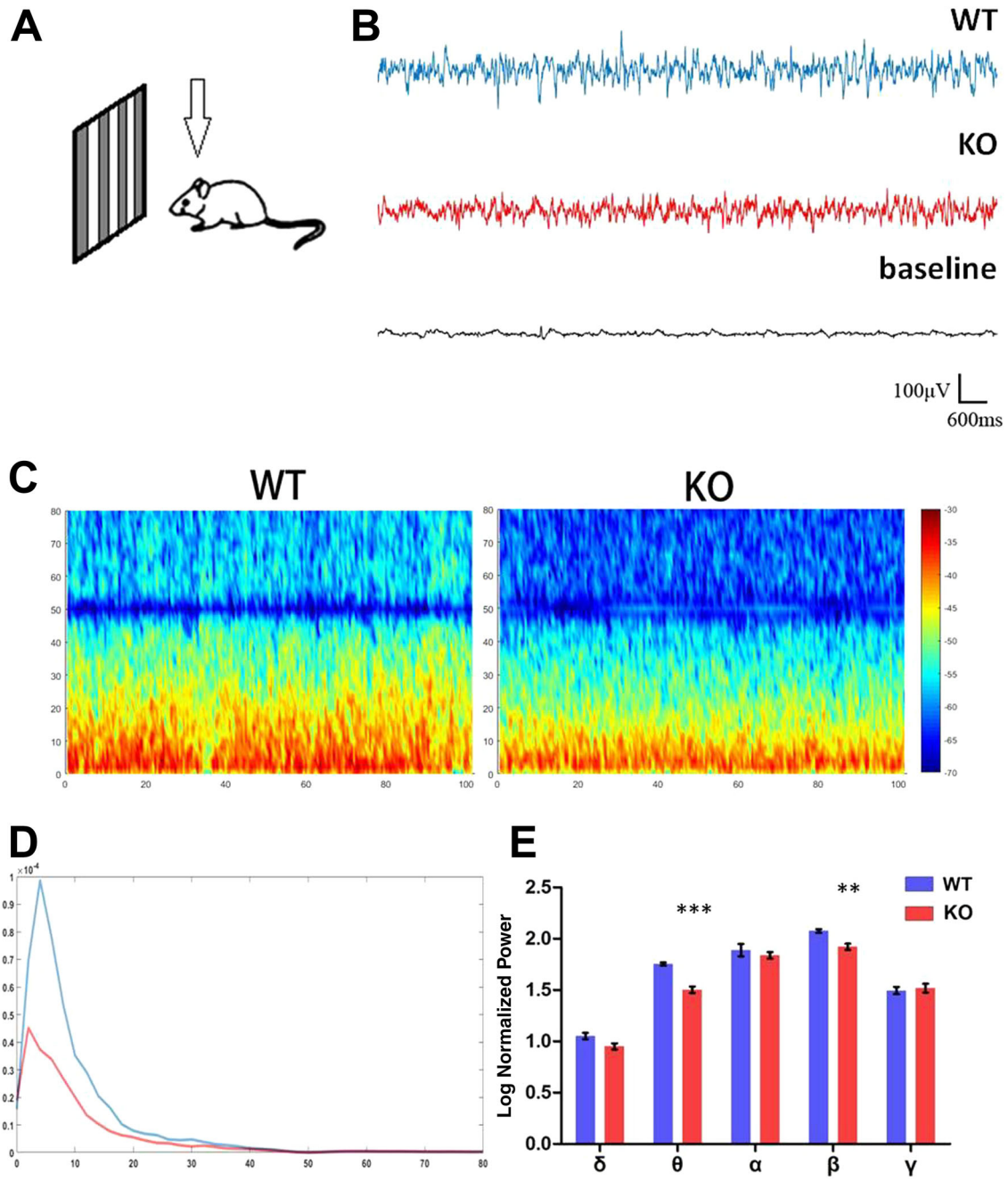

Fig. 6 Dendritic cell factor-knockout (DCF1-KO) mice display decreased theta and beta power in layer 5 of primary visual cortex. **A** Schematic of the cortical recording set-up. **B** Representative local field potentials recorded in layer 5 of V1 in DCF1-KO mice (red), WT mice (blue), and the baseline (black). **C** Representative population power spectrograms from single DCF1-KO and WT mice. **D** Representative Poisson distribution spectrograms from single DCF1-KO and WT mice. Blue, WT mouse; red, DCF1-KO mouse. **E** Bar plots comparing the delta (1–4 Hz), theta (4–8 Hz), alpha (8–15 Hz), beta (15–30 Hz), and gamma (30–100Hz) power after visual stimulation in DCF1-KO and WT mice (**$P < 0.01$, ***$P < 0.001$, one-way ANOVA; mean ± SE; $n = 3$).

DCF1-KO Mice Show More Visual Activation of GAD67 in Layer 5 of Primary Visual Cortex

To further study the mechanism underlying the visual deficit in DCF1-KO mice, we investigated the visual pathway using c-fos tagging [18–20]. The results indicated that GAD67 co-labeled with c-fos was activated in V1 when DCF1-KO mice were exposed to light daily for 1 h (Fig. 5A) and the number of activated GAD67 neurons differed significantly from the WT (Fig. 5B). Further statistical analysis showed that this increase was mainly located in layer 5 (Fig. 5C). This finding supports the hypothesis that abnormally increased GAD67 results in the visual deficit in DCF1-KO mice.

DCF1-KO Mice Display Decreased Theta and Beta Power in Layer 5 of Primary Visual Cortex

The increase in GABAergic neurons in layer 5 of V1 may lead to low local field potentials (LFPs). So, we tested the LFPs in layer 5 of V1 by recording during visual stimulation (Fig. 6A–C). The results showed lower theta (4–8 Hz), and beta (15–30 Hz) power in the DCF1-KO mice than in the WT mice (Fig. 6D, E), which explained the visual deficit revealed by the behavioral tests.

DCF1-KO Mice Show Rescued Visual Behavior after Inhibition of GABA

As the visual deficit in the DCF1-KO mice was probably caused by the abnormally increased GAD67, we thus attempted to induce recovery of the visual defect by reducing the GABA expression. GABA was suppressed by Ginkgolide A, which was diluted in DMSO and normal saline. Surprisingly, we found that the visual deficit in DCF1-KO mice was partially rescued after inhibition of GABA, as assessed by the visual tracking assay (Fig. 7A) and the visual water test (Fig. 7B). Further, we recorded LFPs in GABA-inhibited mice (Fig. 8A) and found that the theta and beta oscillations were also restored (Fig. 8B, C). These results support the hypothesis that the visual deficit in DCF1-KO mice was due to the GABA system.

Discussion

In this study, we found that DCF1-KO mice had a visual deficit and confirmed this in two visual behavioral tests. We also carried out Western blotting, immunohistochemistry, and electrophysiology. Then we tested mice in which GABA was inhibited by Ginkgolide A, and found that the visual deficit was partially rescued. Our results revealed that DCF1-KO mice presented a visual behavioral deficit,

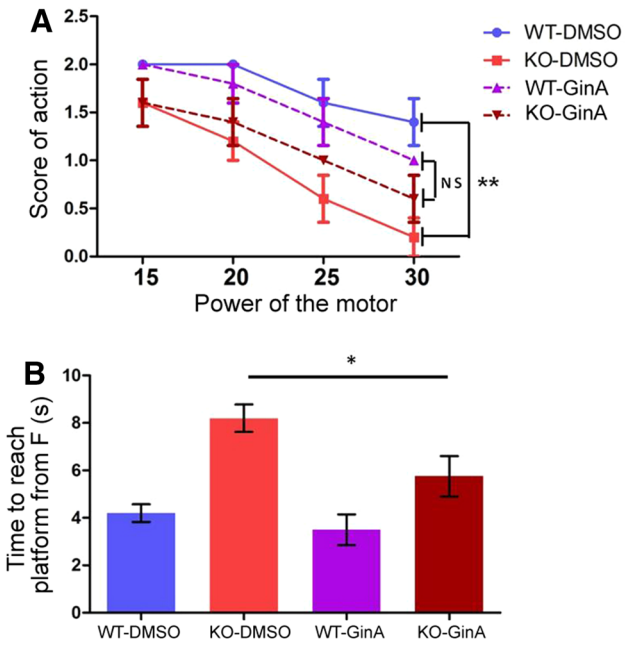

Fig. 7 Suppression of GABA rescues the visual defect in DCF1-KO mice. **A** DCF1-KO mice injected with Ginkgolide A (GinA) scored higher in visual tracking than DCF1-KO mice injected with DMSO (**$P < 0.01$, one-way ANOVA; mean ± SE; $n = 6$). **B** Time to reach the platform. DCF1-KO mice injected with GinA took less time to reach the platform from the far side position than those injected with DMSO (*$P < 0.05$, one-way ANOVA; mean ± SE; $n = 6$).

higher GAD67 levels, and lower electrophysiological activity in V1 *via* the GABA system.

Inhibition in V1 has been proposed to control sensitivity and mediate competition between stimuli. The responsiveness of V1 neurons decreases when the contrast of an optimal stimulus increases (contrast saturation) or when an orthogonal stimulus is superimposed (cross-orientation suppression) [3]. These phenomena are collectively known as contrast gain control, or normalization [21, 22]. They have been ascribed to inhibition of other cortical neurons by GABA [23–27]. As a lack of DCF1 leads to high levels of GAD67, which mainly synthesizes GABA, it could result in a poorer response to a visual stimulus in DCF1-KO mice and suggests an as-yet unknown association between DCF1 and GABA.

Cortical oscillations are classified based on frequency into delta (1–4 Hz), theta (4–8 Hz), alpha (8–12 Hz), beta (10–30 Hz), and gamma (30–100 Hz) bands [28]. Our results showed that theta and beta power in the DCF1-KO mice was lower than that in WT mice, which may be due to increased GABA in V1. Theta oscillations play a significant role monitoring regular movement [29]. Working memory-related oscillations in the theta band have been found in the monkey visual cortex and are correlated with the behavioral performance on a contrast discrimination task [30]. We consider that low theta power results in a poor ability to identify details. Low

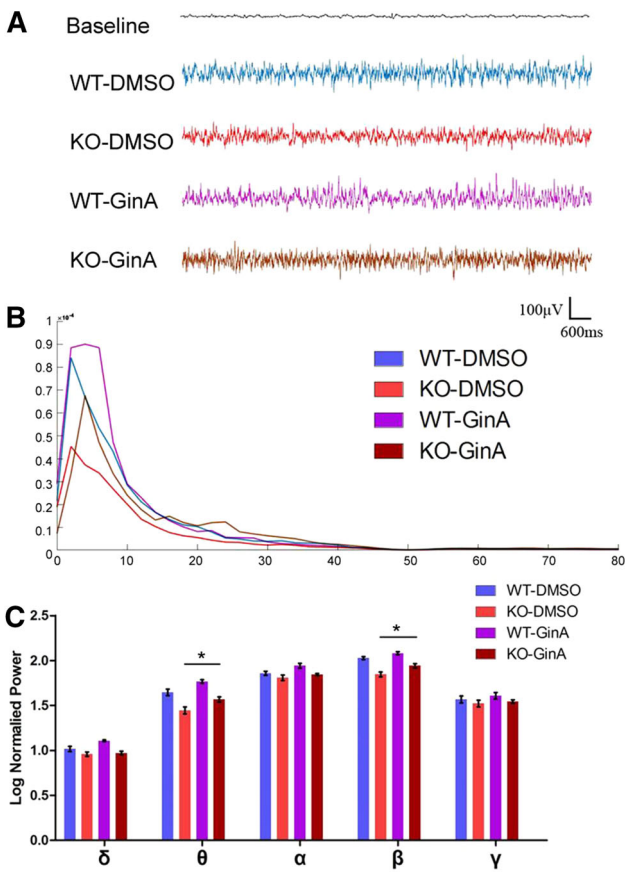

Fig. 8 DCF1-KO mice display rescued theta and beta power. **A** Representative LFPs recorded in layer 5 of V1 at baseline (black), and in WT mice injected with DMSO (blue), DCF1-KO mice injected with DMSO (red), WT mice injected with GinA (purple), and DCF1-KO mice injected with GinA (brown). **B** Representative Poisson distribution spectrograms from single mice. Blue, WT mouse injected with DMSO; red, DCF1-KO mouse injected with DMSO; purple, WT mouse injected with GinA; brown, DCF1-KO mouse injected with GinA. **C** Bar plots of log normalized power for delta (1–4Hz), theta (4–8 Hz), alpha (8–15 Hz), beta (15–30 Hz), and gamma (30–80Hz) oscillations upon visual stimulation in WT mice injected with DMSO (blue), DCF1-KO mice injected with DMSO (red), WT mice injected with GinA (purple), and DCF1-KO mice injected with GinA (brown) (*$P < 0.05$, one-way ANOVA; mean ± SE; $n = 3$).

theta power resulted in poor performance in the head-tracking assay. Beta oscillations play an important role in coding [31]. The low beta power we recorded resulted in poor visual signal processing.

Acknowledgements This work was supported by the National Natural Science Foundation of China (81271253 and 81471162), the Science and Technology Commission of Shanghai Municipality, China (14JC1402400), and the Key Innovation Project of Shanghai Municipal Education Commission, China (14ZZ090).

Compliance with Ethical Standards

Conflict of interest All authors claim that there are no conflicts of interest.

References

1. Sarihi A, Mirnajafi-Zadeh J, Jiang B, Sohya K, Safari MS, Arami MK, *et al.* Cell type-specific, presynaptic LTP of inhibitory synapses on fast-spiking GABAergic neurons in the mouse visual cortex. J Neurosci 2012, 32: 13189–13199.
2. Kirmse K, Kirischuk S. Ambient GABA constrains the strength of GABAergic synapses at Cajal-Retzius cells in the developing visual cortex. J Neurosci 2006, 26: 4216–4227.
3. Katzner S, Busse L, Carandini M. GABAA inhibition controls response gain in visual cortex. J Neurosci 2011, 31: 5931–5941.
4. Pinal CS, Tobin AJ. Uniqueness and redundancy in GABA production. Perspect Dev Neurobiol 1998, 5: 109–118.
5. Soghomonian JJ, Martin DL. Two isoforms of glutamate decarboxylase: why? Trends Pharmacol Sci 1998, 19: 500–505.
6. Asada H, Kawamura Y, Maruyama K, Kume H, Ding RG, Kanbara N, *et al.* Cleft palate and decreased brain gamma-aminobutyric acid in mice lacking the 67-kDa isoform of glutamic acid decarboxylase. Proc Natl Acad Sci U S A 1997, 94: 6496–6499.
7. Liu Q, Feng R, Chen Y, Luo G, Yan H, Chen L, *et al.* Dcf1 Triggers dendritic spine formation and facilitates memory acquisition. Mol Neurobiol 2017. doi: https://doi.org/10.1007/s12035-016-0349-6.
8. Wen T, Gu P, Chen F. Discovery of two novel functional genes from differentiation of neural stem cells in the striatum of the fetal rat. Neurosci Lett 2002, 329: 101–105.
9. Li X, Feng R, Huang C, Wang H, Wang J, Zhang Z, *et al.* MicroRNA-351 regulates TMEM 59 (DCF1) expression and mediates neural stem cell morphogenesis. RNA Biol 2012, 9: 292–301.
10. Wang L, Wang J, Wu Y, Wu J, Pang S, Pan R, *et al.* A novel function of dcf1 during the differentiation of neural stem cells in vitro. Cell Mol Neurobiol 2008, 28: 887–894.
11. Thaung C, Arnold K, Jackson IJ, Coffey PJ. Presence of visual head tracking differentiates normal sighted from retinal degenerate mice. Neurosci Lett 2002, 325: 21–24
12. Leitner FC, Melzer S, Lutcke H, Pinna R, Seeburg PH, Helmchen F, *et al.* Spatially segregated feedforward and feedback neurons support differential odor processing in the lateral entorhinal cortex. Nat Neurosci 2016, 19: 935–944.
13. Bokil H, Andrews P, Kulkarni JE, Mehta S, Mitra PP. Chronux: A platform for analyzing neural signals. J Neurosci Methods 2010, 192: 146–151.
14. Watanabe M. Glutamate signaling and neural plasticity. No To Hattatsu 2013, 45: 267–274.
15. Irwin RP, Allen CN. GABAergic signaling induces divergent neuronal Ca^{2+} responses in the suprachiasmatic nucleus network. Eur J Neurosci 2009, 30: 1462–1475.
16. Jiang L, Kundu S, Lederman JD, Lopez-Hernandez GY, Ballinger EC, Wang S, *et al.* Cholinergic signaling controls conditioned fear behaviors and enhances plasticity of cortical-amygdala circuits. Neuron 2016, 90: 1057–1070.
17. Chattopadhyaya B, Di Cristo G, Wu CZ, Knott G, Kuhlman S, Fu Y, *et al.* GAD67-mediated GABA synthesis and signaling regulate inhibitory synaptic innervation in the visual cortex. Neuron 2007, 54: 889–903.
18. Pothuizen HH, Davies M, Albasser MM, Aggleton JP, Vann SD. Granular and dysgranular retrosplenial cortices provide qualitatively different contributions to spatial working memory: evidence from immediate-early gene imaging in rats. Euro J Neurosci 2009 30: 877–888.
19. Yamada Y, Hada Y, Imamura K, Mataga N, Watanabe Y, Yamamoto M. Differential expression of immediate-early genes, c-fos and zif268, in the visual cortex of young rats: Effects of a

noradrenergic neurotoxin on their expression. Neuroscience 1999, 92: 473–484.
20. Zhu XO, McCabe BJ, Aggleton JP, Brown MW. Mapping visual recognition memory through expression of the immediate early gene c-fos. Neuroreport 1996, 7: 1871–1875.
21. Heeger DJ. Normalization of cell responses in cat striate cortex. Vis Neurosci 1992, 9:181–197.
22. Busse L, Wade A, Carandini M. Representation of concurrent stimuli by population activity in visual cortex. Neuron 2009, 64: 931–942
23. Bonds AB. Role of inhibition in the specification of orientation selectivity of cells in the cat striate cortex. Vis Neurosci 1989, 2: 41–55.
24. Carandini M HD. Summation and division by neurons in primate visual cortex. Science 1994, 264: 1333–1336.
25. Carandini M HD, Movshon JA. Linearity and normalization in simple cells of the macaque primary visual cortex. J Neurosci 1997, 17: 8621–8644.
26. Morrone MC, Burr DC, Maffei L. Functional implications of cross-orientation inhibition of cortical visual cells. I. Neurophysiological evidence. Proc R Soc Lond B Biol Sci 1982, 216: 335–354.
27. Somers DC, Todorov EV, Siapas AG, Toth LJ, Kim DS, Sur M. A local circuit approach to understanding integration of long-range inputs in primary visual cortex. Cereb Cortex 1998, 8: 204–217.
28. Sohal VS. Insights into cortical oscillations arising from optogenetic studies. Biol Psychiatry 2012, 71: 1039–1045.
29. Biau E, Torralba M, Fuentemilla L, de Diego Balaguer R, Soto-Faraco S. Speaker's hand gestures modulate speech perception through phase resetting of ongoing neural oscillations. Cortex 2015, 68: 76–85.
30. Rainer G, Lee H, Simpson GV, Logothetis NK. Working-memory related theta (4–7 Hz) frequency oscillations observed in monkey extrastriate visual cortex. Neurocomputing 2004, 58-60: 965–969.
31. Schubert JT, Buchholz VN, Focker J, Engel AK, Roder B, Heed T. Oscillatory activity reflects differential use of spatial reference frames by sighted and blind individuals in tactile attention. Neuroimage 2015, 117: 417–428.